

Interleukin-12 Deficiency Is Permissive for Angiogenesis in UV Radiation-Induced Skin Tumors

Syed M. Meeran,¹ Suchitra Katiyar,¹ Craig A. Elmetts,^{1,2,3} and Santosh K. Katiyar^{1,2,3}

¹Department of Dermatology and ²Skin Diseases Research Center, University of Alabama at Birmingham; ³Birmingham Veterans Affairs Medical Center, Birmingham, Alabama

Abstract

We have shown previously that endogenous deficiency of interleukin (IL)-12 promotes photocarcinogenesis in mice. To characterize the role of IL-12 deficiency in tumor angiogenesis, we developed IL-12p35 knockout (IL-12 KO) mice on a C3H/HeN background. IL-12 KO mice and their wild-type (WT) counterparts were subjected to a photocarcinogenesis protocol. When tumor yield was stabilized, samples of tumor and tumor-uninvolved UVB-exposed skin were collected and subjected to immunohistochemistry, gelatinolytic zymography, real-time PCR, and Western blot analysis of angiogenic factors. We found that the protein, mRNA expression and/or activity of the matrix metalloproteinases (MMP)-2, MMP-3, MMP-7, and MMP-9, and basic fibroblast growth factor, which play crucial roles in tumor growth, were significantly higher in UVB-exposed skin and tumors of IL-12 KO mice compared with WT mice. With respect to the tumor vasculature, the expression of CD31-positive cells and the expression of vascular endothelial growth factor were higher in the tumors of IL-12 KO mice than WTs. The proliferative capacity of tumor cells of the IL-12 KO mice was significantly higher than their WT counterparts when determined by 3-(4,5-dimethylthiazol-2-yl)-2,5-diphenyltetrazolium bromide assay and by analyzing the expression of cyclin D1. The level of the proinflammatory cytokine IL-6 and the expression of IL-23 in tumors of IL-12 KO mice were markedly higher than in the tumors of WT mice. IL-23 has been shown to promote tumor growth. Together, these data indicate for the first time that IL-12 deficiency promotes proangiogenic stimuli in UVB-induced skin tumors and suggest that endogenous enhancement of IL-12 levels may be effective in the prevention and treatment of UV-induced skin cancers. [Cancer Res 2007;67(8):3785–93]

Introduction

Solar UV radiation, particularly UVB (290–320 nm) component, acts as a tumor initiator, tumor promoter, and a complete carcinogen, therefore responsible for higher risk of melanoma and nonmelanoma skin cancers in humans (1, 2). UV radiation induces immunosuppressive effects, which are considered to be a risk factor for the development of melanoma and nonmelanoma skin cancers (3, 4). It has been shown that the immunoregulatory cytokine interleukin (IL)-12 has the ability to inhibit the immunosuppressive effects of UV radiation (5, 6). IL-12 has been

shown to have antitumor activity in a wide variety of murine tumor models (7–10) and its presence at tumor site is critical for tumor regression (11). We have shown previously that mice deficient in IL-12 are at higher risk of UV radiation-induced skin tumors than their wild-type (WT) counterparts (12). We observed that the development of UV-induced tumors was more rapid and the tumor multiplicity and tumor size were significantly higher in IL-12p35 knockout (IL-12 KO) mice than C3H/HeN mice, their WT counterparts, after exposure to a complete photocarcinogenesis protocol. Moreover, the malignant transformation of UVB-induced papillomas to carcinomas was higher in the IL-12 KO mice in terms of carcinoma incidence, multiplicity, and size (12). These data suggested that deficiency of IL-12 in mice increases susceptibility to photocarcinogenesis.

The demonstration of significant antitumor activity in several preclinical animal tumor models has stimulated interest in the therapeutic use of IL-12 (13–15) but our understanding of the mechanisms underlying the antitumor activity of IL-12 is incomplete. It has been reported that IL-12 inhibits angiogenesis in mammary tumors (16); however, this effect has not been examined in UVB-induced skin tumors. Our previous observation that the UVB-induced skin tumors of IL-12 KO mice were larger in size than the tumors of their WT counterparts suggested that the deficiency of IL-12 might promote angiogenesis in the UVB-induced skin tumors.

To determine whether IL-12 deficiency promotes tumor angiogenesis in the photocarcinogenesis model, female IL-12 KO and their WT mice were subjected to photocarcinogenesis protocol (1, 12). At 35 weeks of UVB irradiation, when the tumor yield was stabilized, mice were sacrificed. Tumor samples and tumor-uninvolved UVB-exposed skin samples were collected to characterize the role of IL-12 on angiogenesis in UVB-induced skin tumors and data were compared with skin samples from age- and sex-matched WT mice that were not UVB irradiated. Analyses included the determination of CD31 and vascular endothelial growth factor (VEGF), which are expressed on the surface of endothelial cells and have been implicated in the formation of new blood vasculature in growing tumors (17, 18). The expression of VEGF promotes proliferation (19, 20) and survival of endothelial cells in newly formed vessels (20, 21). The expression and activity of matrix metalloproteinases (MMP), which degrade the extracellular matrix and contribute to angiogenesis, tumor growth, and invasion (22), was determined. Additionally, we determined the levels of IL-23, which promotes tumor growth, and the proliferative capacity of the tumor cells using an *in vitro* 3-(4,5-dimethylthiazol-2-yl)-2,5-diphenyltetrazolium bromide (MTT) assay and Western blotting of cyclin D1.

Materials and Methods

Antibodies and chemicals. Monoclonal antibodies specific for CD31 (platelet/endothelial cell adhesion molecule 1), VEGF, basic fibroblast growth factor (bFGF), and IL-6 as well as secondary antibody conjugated to

Requests for reprints: Santosh K. Katiyar, Department of Dermatology, University of Alabama at Birmingham, 1670 University Boulevard, Volker Hall 557, P.O. Box 202, Birmingham, AL 35294. Phone: 205-975-2608; Fax: 205-934-5745; E-mail: skatiyar@uab.edu.

©2007 American Association for Cancer Research.
doi:10.1158/0008-5472.CAN-06-3134

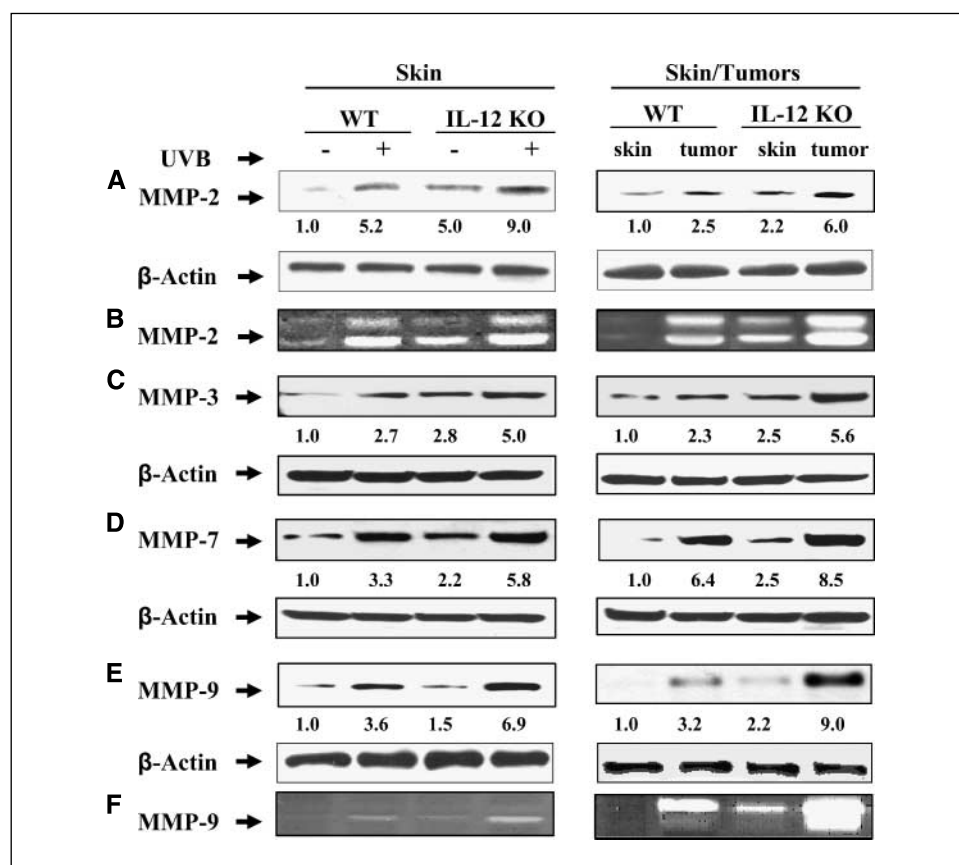


Figure 1. IL-12 KO mice express higher levels of MMPs in chronic UVB-exposed skin and tumors compared with their WT counterparts. At the termination of the photocarcinogenesis protocol at 35 wks, the tumors and UVB-exposed skin samples were collected and the levels of MMPs were analyzed by Western blot analysis and gelatinolytic zymography. Representative Western blots of MMP-2 (A), MMP-3 (C), MMP-7 (D), and MMP-9 (E) from WT and IL-12 KO mice from experiments conducted in skin or tumor samples from at least six mice independently from each treatment group which showed identical patterns. Skin samples from age-matched mice that were not UVB irradiated were included in this assay as a control. The activity of MMP-2 (B) and MMP-9 (F) proteins was determined by gelatinolytic zymography in the samples as described in Materials and Methods. The densitometric data (arbitrary) of each band of the blot are shown under the immunoblots in terms of fold change. Equal protein loading was confirmed by analysis of β -actin.

phycoerythrin-Cy5 were purchased from BD Biosciences PharMingen (San Diego, CA). Antibodies specific for MMP-2, MMP-3, MMP-7, MMP-9, Cip1/p21, Kip1/p27, and IL-23 were purchased from Santa Cruz Biotechnology, Inc. (Santa Cruz, CA). The manufacturer-supplied standardized real-time PCR primer pairs for the MMP-2, MMP-3, MMP-7, MMP-9, VEGF, bFGF, IL-23p19, and β -actin were obtained from the SuperArray Bioscience Corp. (Frederick, MD). All other chemicals were purchased from Sigma Chemical Co. (St. Louis, MO).

Animals. IL-12 KO mice on a C57BL/6 genetic background and C3H/HeN mice (6–7 weeks old) were obtained from The Jackson Laboratory (Bar Harbor, ME). The IL-12 KO mice were backcrossed with C3H/HeN mice to generate IL-12 KO mice on a C3H/HeN background in our Animal Resource Facility as described previously (12). The mutation in the p35 chain of the IL-12 protein molecule in IL-12 KO mice completely eliminates the synthesis of biologically active IL-12 protein in these mice. All mice were maintained under the following conditions: 12-h dark/12-h light cycle, $24 \pm 2^\circ\text{C}$ temperature, and $50 \pm 10\%$ relative humidity. The mice were fed Purina Taklad diet (Harlan Teklad, Madison, WI) and water *ad libitum*. The animal protocol was approved by Institutional Animal Care and Use Committee of the University of Alabama at Birmingham (Birmingham, AL).

Photocarcinogenesis protocol. Female mice of equivalent age (6–8 weeks) were used in this study. The IL-12 KO mice on C3H/HeN background and their WT (C3H/HeN) counterparts were divided into two treatment groups separately with 20 mice in each group. One group was treated as a control (non-UVB exposed) and a second group of mice was exposed to photocarcinogenesis protocol. At least 48 h before UVB exposure, the backs of the mice were shaved with electric clippers and treated with Nair depilatory lotion. The groups of mice that were not exposed to UVB also were shaved, and depilatory lotion was applied to maintain a similar treatment protocol. Mice were UVB irradiated as described earlier (23, 24). Briefly, the shaved dorsal skin was exposed to UV radiation from a band of four FS24T1 UVB lamps (Daavlin, UVA/UVB Research Irradiation Unit, Bryan, OH) equipped with an electronic

controller to regulate UV dosage. The UVB lamps primarily emit UVB (290–320 nm, >80% of total energy) and UVA (320–375 nm, <20% of total energy) radiation with peak emission at 314 nm as monitored (23). The UVB emission also was monitored regularly with an IL-1700 phototherapy radiometer (International Light, Newburyport, MA).

A photocarcinogenesis protocol was used as described previously (12, 23), in which mice were UVB irradiated everyday (180 mJ/cm^2) for a total of 10 days to stimulate tumor initiation. To stimulate tumor promotion, 1 week after the last UVB exposure of the tumor initiation stage, the mice were again irradiated with the same dose of UVB thrice weekly until the end of the protocol. The UVB-irradiated dorsal skin of the mice was examined on a weekly basis for papillomas or tumor appearance. Growths >1 mm in diameter and that persisted for at least 2 weeks were defined as tumors and recorded. Tumor data for each mouse were recorded until the yield and size stabilized. Control groups of mice, which were age and sex matched with the experimental groups, were not exposed to UVB.

Preparation of tumor and skin lysates and Western blotting. Lysates for Western blot analysis were prepared from tumor and age matched non-UVB-exposed skin biopsies as described previously (25, 26). The UVB-exposed skin sites away from the tumors (i.e., tumor uninvolved site) were also used for the analysis. The tissue samples were pooled from at least two mice in each group, and five sets of pooled samples from each treatment group were used to prepare lysates, thus $n = 10$. Western blot analysis was done to determine the levels of MMP-2, MMP-3, MMP-7, MMP-9, VEGF, bFGF, IL-6, and IL-23 as described previously (25). Briefly, proteins (25–50 μg) were resolved on 10% to 12% SDS-polyacrylamide gel and transferred onto nitrocellulose membranes. Membranes were incubated in blocking buffer for 1 h at room temperature and then incubated with the primary antibodies in blocking buffer overnight at 4°C . The membrane was then washed with PBS and incubated with secondary antibody conjugated with horseradish peroxidase. Protein bands were visualized using the enhanced chemiluminescence detection system (Amersham Life Science, Inc., Piscataway, NJ). To verify equal protein loading and transfer of proteins

from gel to membrane, the blots were stripped and reprobed for β -actin using an anti-actin rabbit polyclonal antibody.

Gelatinolytic zymography for MMP-2 and MMP-9. The activity of MMP-2 and MMP-9 proteins in tumor or skin homogenates was analyzed by gelatinolytic zymography using SDS-PAGE as described by us previously (25). Briefly, the samples (30–40 μ g protein) were loaded on an electrophoresis gel copolymerized with 0.1% gelatin. After electrophoresis, the gels were washed to remove the SDS, rinsed with zymogen activation buffer, and then incubated for 18 h at 37°C in the same buffer. After washing, the gels were stained for 2 h with PhastGel Blue R stain and destained.

RNA extraction and quantitative real-time PCRs. The total RNA was extracted from the mouse skin or tumor samples using Trizol reagent (Invitrogen, Carlsbad, CA) following the protocol recommended by the manufacturer. Briefly, skin or tumor samples were homogenized with Trizol reagent using Teflon homogenizer (Fisher Scientific, Pittsburgh, PA). The homogenate was centrifuged at $12,000 \times g$ for 10 min at 4°C and the resulting supernatant was mixed with chloroform, and aqueous phase was separated. The RNA was precipitated by mixing the equal amounts of the aqueous phase and the isopropanol. The sample was shaken, incubated for 20 min at room temperature, and centrifuged again as described previously. The precipitate was washed with 75% ethanol in diethyl pyrocarbonate-treated RNase-free water and stored at -70°C. The concentration of total RNA was determined by measuring the absorbance at 260 nm using Beckman Coulter (Fullerton, CA) DU 530 spectrophotometer.

The mRNA expression of MMPs, VEGF, and IL-23p19 in skin and tumor samples was determined using real-time PCR. For the mRNA quantification, cDNA was synthesized using 3 μ g RNA through a reverse transcription reaction (iScript cDNA Synthesis kit, Bio-Rad, Hercules, CA). Using SYBR Green/Fluorescein PCR Master Mix (SuperArray Bioscience), cDNA was amplified using real-time PCR with a Bio-Rad MyiQ thermocycler and SYBR Green detection system (Bio-Rad). Samples were run in triplicate to ensure amplification integrity. Manufacturer-supplied primer pairs were used to measure the following: MMP-2, MMP-3, MMP-7, MMP-9, VEGF, IL-23p19, and β -actin. The standard PCR conditions were 95°C for 15 min and then 40 cycles at 95°C for 30 s, 55°C for 30 s, and 72°C for 30 s, as recommended by the primer's manufacturer. The expression levels of genes were normalized to the expression level of the β -actin mRNA in each sample. The threshold for positivity of real-time PCR was determined based on negative controls. For mRNA analysis, the calculations for determining the relative level of gene expression were made using the cycle threshold (C_t) method. The mean C_t values from duplicate measurements were used to calculate the expression of the target gene with normalization to a housekeeping gene used as internal control (β -actin) and using the $2^{-\Delta C_t}$ formula.

Immunohistochemical assessment of CD31. The expression of CD31 was determined by immunostaining as described previously (25). Briefly, frozen sections (5 μ m thick) were fixed in cold acetone and nonspecific binding sites were blocked by immersing the sections in Tris-HCl buffer containing 5% goat serum and bovine serum albumin (0.5% w/v). The sections were then incubated with monoclonal antibodies specific for CD31 for 1 h. Antibody binding was detected by subsequent incubation of sections with streptavidin-phycoerythrin-Cy5 secondary antibody for 1 h. After washing, the sections were counterstained with Hoechst 33342, which stains nuclei. The intensity of the staining was evaluated using a microscope equipped for immunofluorescence analysis. Peritumoral vascular density was assessed by localizing the immunostaining by three independent observers blinded to the treatment group.

Proliferation assay in tumor cells. The proliferative potential of tumor cells obtained from IL-12 KO and WT mice was assessed using the MTT assay. Tumor cell lines with biological activity were established using the Cancer Cell Isolation kit from Panomics (Redwood City, CA) following the manufacturer's protocol. Briefly, tumor pieces of <2 mm³ size were seeded into six-well culture plates and cultured in RPMI 1640 supplemented with 20% fetal bovine serum, 1% L-glutamine, 1% MEM nonessential amino acid, and 1% antibiotic/penicillin-streptomycin solution. Cells were maintained at 37°C in a humidified atmosphere containing 5% CO₂. Cells were

harvested with 0.1% trypsin/0.05% EDTA when the cultures had reached ~80% confluence. These cells were used for three to four subsequent passages and thereafter used for determining the proliferative potential of the cells (2×10^4 per well) using the MTT proliferation assay as described previously (27).

Densitometry and statistical analysis. The susceptibility of IL-12 KO mice to tumors caused by UV radiation was compared with the susceptibility of WT mice. The data were collected in an aggregate form >35 weeks. A linear model was fit to each of the outcome variables. The independent variables in the model were group, time, and a group/time interaction term, which helps in testing if the rate of change in the outcome variables over time is a function of the group. The numerical values shown under each Western blot are arbitrary units. In each case, the values for control group is used as "1" and comparison was then made with densitometry values obtained from with or without treatment of UVB radiation in WTs and IL-12 KO mice. The comparative data are presented as fold change after treatment. The statistical significance of difference in between the values of control and treatment groups in Western blot analysis and real-time PCR was determined by Student's *t* test. A *P* value <0.05 was considered statistically significant.

Results

IL-12 KO mice were more susceptible to UV carcinogenesis.

On exposure to the photocarcinogenesis protocol, we confirmed that, as we have reported previously (12), the IL-12 KO mice were more susceptible to photocarcinogenesis than their WT counterparts (Table 1). The total number of tumors in the group of IL-12 KO mice ($n = 20$) was significantly higher than in the WT group (72 versus 42; $P < 0.01$). Similarly, a higher number of tumors per tumor-bearing mouse was observed in the group of IL-12 KO mice than in the WT group. At the termination of the experiment, the tumor volume of each mouse in each group was measured, and it was observed that tumor volume per tumor was significantly higher in the group of IL-12 KO mice than the WT group ($P < 0.001$; Table 1). The greater incidence and, in particular, the greater size of the tumors in the IL-12 KO mice suggested enhanced angiogenesis in the IL-12 KO mice.

IL-12-deficient mice promote higher expression of protein and mRNA levels of MMPs in UV-exposed skin and UV-induced tumors. The protein expression of MMP-2, MMP-3, MMP-7, and

Table 1. Characteristics of UV-induced skin tumors in IL-12-deficient mice and their WT counterparts

Tumor characteristics	Treatment group		% Increase in IL-12 KO
	WT	IL-12 KO	
Tumor incidence (%)	75	90	15
Total no. tumors/group	42	72	42*
Tumors/tumor bearing mouse	2.7 ± 0.6	3.8 ± 0.6	29 [†]
Tumor volume/tumor (mm ³)	12 ± 5	24 ± 4	50*

NOTE: Mice were exposed to UVB (180 mJ/cm²) thrice weekly for a total of 35 wks. Tumor data were recorded at the termination of the experiment. $n = 20$. Control groups of WT and IL-12 KO mice, which were not exposed to UVB, were also maintained. The mice in control groups did not develop tumors during this period.

* $P < 0.001$, significant increase versus WT mice.

[†] $P < 0.05$, Significant increase versus WT mice.

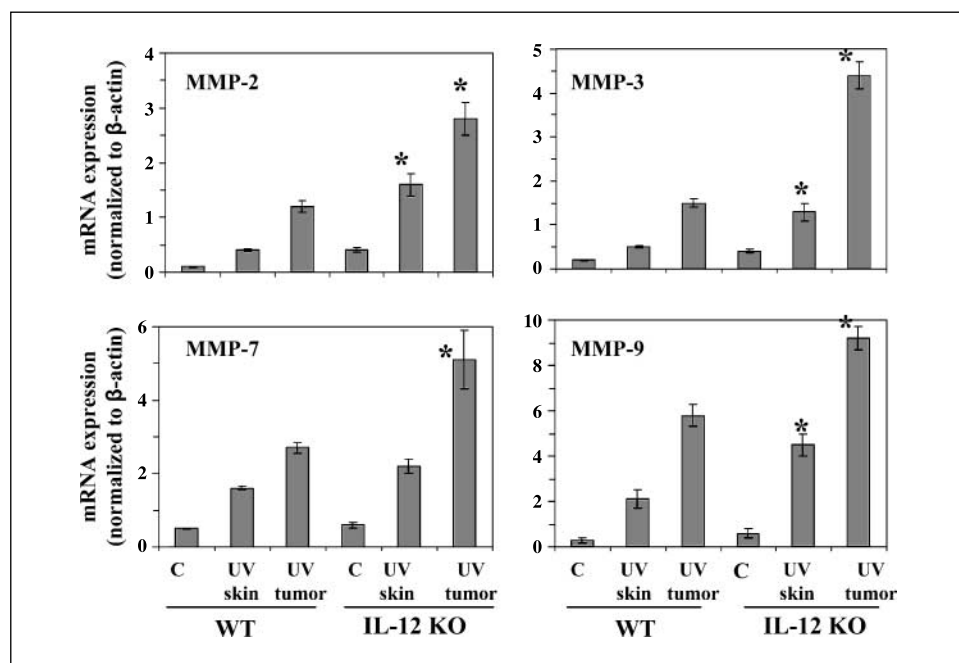


Figure 2. IL-12 KO mice express higher levels of mRNA of MMPs in UVB-exposed skin and tumors compared with their WT mice. At the termination of the photocarcinogenesis experiment at 35 wks, the tumors and UVB-exposed skin samples were collected, total RNA was isolated, and mRNA expression of MMP-2, MMP-3, MMP-7, and MMP-9 was determined using real-time PCR SYBR Green system as described in Materials and Methods. Skin samples from age-matched mice that were not UVB irradiated were used as a control. The results are presented as the expression of the individual mRNA with normalization to β -actin using the C_t method. Columns, mean of at least six tumors or skin samples from six different animals; bars, SD. C, non-UVB-exposed controls. $P < 0.01$, significant difference versus WT.

MMP-9 was analyzed using Western blotting, which indicated higher expression of these MMPs in the UVB-exposed skin of both WT and IL-12 KO mice compared with non-UVB-exposed skin from control mice (Fig. 1A, C, D, and E), with the levels being higher in the UVB-exposed skin of IL-12 KO mice than UVB-exposed skin of WT mice. Additionally, the Western blot results confirmed that the levels of MMP-2, MMP-3, MMP-7, and -9 were markedly higher in the UVB-induced tumors of IL-12 KO mice than the UVB-induced tumors of WT mice. As the activity of MMP-2 (gelatinase A) and MMP-9 (gelatinase B) has been shown to have major roles in tumor growth, invasion, and angiogenesis, we determined the activity of MMP-2 and MMP-9 in these samples. Analysis of the activity of MMP-2 using gelatinolytic zymography assay of skin homogenates (Fig. 1B) indicated that the activity was higher in the homogenates of the UVB-exposed skin of IL-12 KO mice than WT mice and that the activity of MMP-2 was also higher in the UVB-induced tumors of the IL-12 KO mice than the UVB-induced tumors of the WT mice. Importantly, the basal levels of MMP-2 activity were higher in the samples of skin from control IL-12 KO that were not exposed to UVB than the skin from nonexposed, control WT mice. Similarly, the activity of MMP-9 was higher in UVB-exposed skin and UVB-induced tumors in IL-12 KO mice than the UVB-exposed skin and tumors of WT mice (Fig. 1F).

To further support our observations on the expression of UVB-induced MMPs in IL-12 KO and their WT mice, we analyzed the mRNA expression of MMP-2, MMP-3, MMP-7, and MMP-9 using real-time PCR in the skin and tumor samples of IL-12 KO mice and the data were compared with the skin and tumor samples of WT mice. As shown in Fig. 2, the mRNA expression of MMP-2, MMP-3, MMP-7, and MMP-9 was higher in UV-exposed skin and tumors of IL-12 KO mice and WT mice compared with non-UVB-exposed skin from control mice, with the levels being significantly higher ($P < 0.01$) in the UVB-exposed skin and UVB-induced tumors of IL-12 KO mice than UVB-induced skin and tumors of WT mice.

IL-12-deficient mice express higher levels of protein and mRNA of VEGF and bFGF in UVB-induced tumors. There is considerable evidence that VEGF and bFGF play a central role in

tumor-induced angiogenesis, as well as tumor growth and metastasis, and are considered as promising targets for antitumor therapy (28, 29). We therefore analyzed the expression of VEGF and bFGF using Western blot analysis with subsequent measurement of band intensities relative to β -actin. Western blot analysis indicated that chronic UVB exposure enhanced the expression of VEGF in the skin of both WT mice and IL-12 KO mice compared with the expression in non-UVB-exposed skin (Fig. 3A) with the expression of VEGF being significantly higher in the UVB-exposed skin of IL-12 KO mice than the UVB-exposed skin of their WT counterparts ($P < 0.001$; Fig. 3A). Similarly, the expression of VEGF was significantly higher in the UVB-induced tumors of IL-12 KO mice than in the UVB-induced tumors of their WT counterparts ($P < 0.001$; Fig. 3B). Similar to VEGF, the expression level of bFGF was also examined in tumors from IL-12 KO mice and was compared with the tumors of WT. As shown in Fig. 3D, the expression level of bFGF was higher in tumors than normal non-UVB-exposed skin samples of the mice with the expression of bFGF being significantly higher in the UVB-induced tumors of IL-12 KO mice than in the UVB-induced tumors of their WT counterparts ($P < 0.01$). To further support our Western blot data, we also analyzed the mRNA expression of VEGF and bFGF in skin and tumors of IL-12 KO and their WT mice following real-time PCR. As shown in Fig. 3, the mRNA expression of VEGF (Fig. 3C) and bFGF (Fig. 3E) was higher in UV-induced tumors of IL-12 KO mice and WT mice compared with non-UVB-exposed skin from control mice, with the levels being significantly higher ($P < 0.01$) in the UVB-induced tumors of IL-12 KO mice than UVB-induced tumors of WT mice.

IL-12-deficient mice exhibit enhanced peritumoral vascular density and enhanced expression of CD31 in UVB-induced tumors. We assessed the extent of neovascularization of the tumors by examination of the expression of CD31, which is known to contribute to the formation of new vasculature and is used as a biomarker of angiogenesis (17). The intensity of the CD31 immunofluorescent staining in the UVB-induced tumors in both IL-12 KO and WT mice was markedly higher than that of non-UVB-exposed control skin. Moreover, the intensity of CD31

staining was markedly higher in the UVB-induced tumors of IL-12 KO mice compared with the UVB-induced tumors of the WT mice (Fig. 4). The observation of localization of the CD31-positive immunofluorescent staining by independent investigators confirmed that the peritumoral vascular density was greater and the numbers of clusters and elongated structures of vessels were higher in the UVB-induced tumors of the IL-12 KO mice compared with the UVB-induced tumors of the WT mice (Fig. 4).

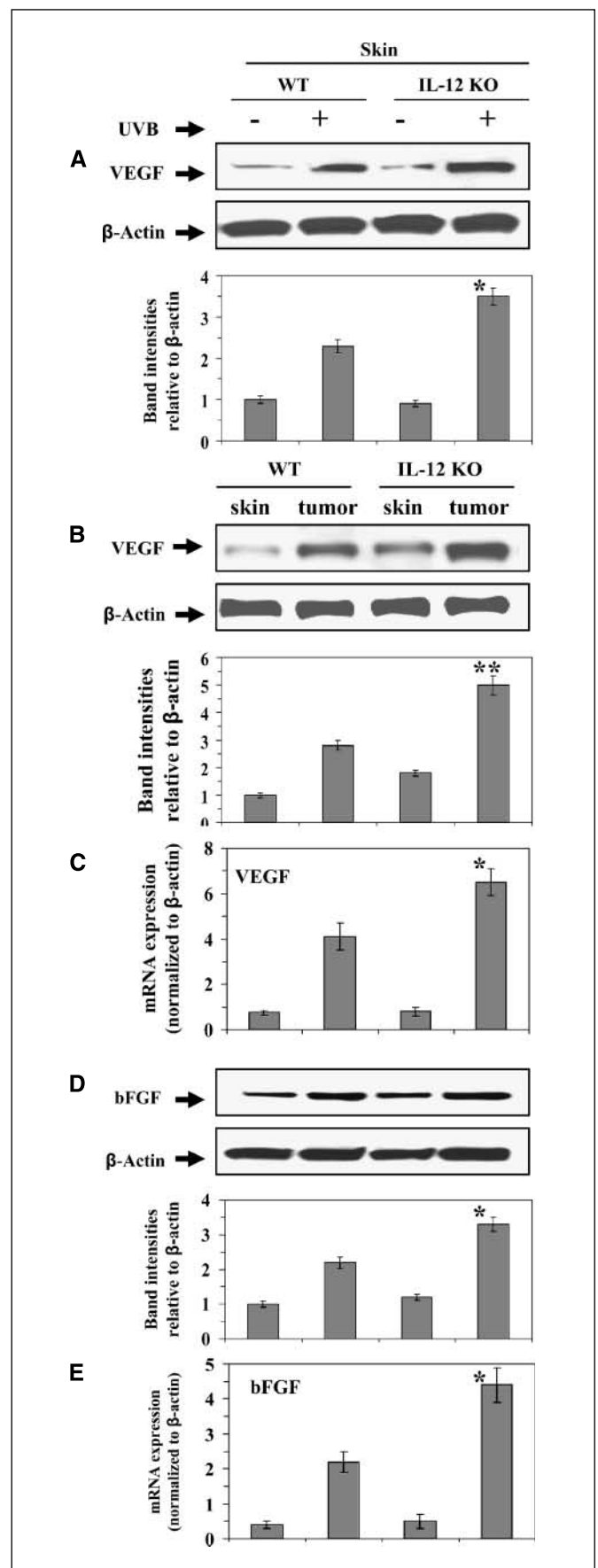
Proliferation of tumor cells *in vitro*. Tumor samples were collected from the IL-12 KO and WT mice when tumor yield was stabilized and tumor cells were isolated and cultured, and the cells were subjected to a MTT proliferation assay (27), which was done at 0, 3, and 5 days after seeding in 96-well culture plates. The proliferative capacity of the cultured tumor cells obtained from IL-12 KO mice was significantly higher ($P < 0.05-0.01$) than that of the cultured tumor cells obtained from the tumors of WT mice (Fig. 5A).

In addition, the levels of expression of the proliferation-specific protein cyclin D1 were estimated by Western blot analysis of tumor cell lysates (Fig. 5B). The expression levels of cyclin D1 were higher in the UVB-induced tumors than the age-matched skin samples from respective control mice, with the levels of cyclin D1 being markedly higher in the UVB-induced tumors of IL-12 KO mice than the UVB-induced tumors of their WT counterparts. As the expression level of cyclin D1 was higher in the tumor cells of IL-12 KO mice than WT, we were interested to examine whether cell cycle checkpoints are intact in IL-12 KO mice. As shown in Fig. 5B, the levels of cell cycle inhibitory proteins Cip1/p21 and Kip1/p27 were analyzed in tumor samples from IL-12 KO mice and WT mice and data were compared with the normal non-UVB-exposed skin samples. Western blot analysis revealed the normal or intact levels of Cip1/p21 and Kip1/p27 in the non-UVB-exposed normal skin samples from both IL-12 KO mice and WT mice; however, the levels of these inhibitory proteins were markedly decreased in tumor samples compared with normal skin samples with the expression of Cip1/p21 and Kip1/p27 being markedly decreased in the tumor samples of IL-12 KO mice than WT mice, suggesting the susceptibility of IL-12 KO mice toward photocarcinogenesis.

Levels of proinflammatory cytokine IL-6 was higher in the tumors of IL-12 KO mice than WT mice. Western blot analysis indicated that the levels of IL-6 in the UVB-induced tumors were higher than the levels in control skin samples and also that the levels of IL-6 in the tumors of IL-12 KO mice were higher than the levels of IL-6 in the tumors of WT mice (Fig. 5C).

IL-12 deficiency promotes IL-23 production in tumors. IL-23, as well as IL-12, is a member of a small family of proinflammatory heterodimeric cytokines (30). These cytokines share a common p40 subunit that is linked covalently either to a p35 subunit to form IL-12 or to a p19 subunit to form IL-23 (31). IL-23 has been shown to promote both tumor incidence and growth through the stimulation of inflammatory responses, such as up-regulation of the MMP-9, and to enhance angiogenesis (32). As shown in Fig. 6, Western blot analysis indicated that the levels of IL-23 were higher

Figure 3. The expression levels of VEGF (A–C) and bFGF (D and E) after chronic exposure to UVB were determined using Western blot analysis and real-time PCR in skin or tumor samples from IL-12 KO and their WT mice, and data were compared with the skin samples from age-matched non-UVB-exposed control mice. Representative examples of blots and the data from real-time PCR are shown from five sets of experiments. The samples in each set were prepared by pooling the skin or tumor samples from two different mice which showed identical pattern ($n = 10$). *, $P < 0.01$; **, $P < 0.001$, significant difference from WT mice.



in the UVB-induced tumors of both WT and IL-12 KO mice than the basal levels of IL-23 in the skin of the corresponding non-UVB-exposed control mice. Indeed, IL-23 was barely detectable in the skin of unexposed mice. Furthermore, the level of IL-23 was higher (>2-fold) in the UVB-induced tumors of IL-12 KO mice than the UVB-induced tumors of their WT counterparts. To support our observation obtained from Western blot analysis, we further determined the expression level of mRNA in these samples using real-time PCR. We found that the mRNA expression of IL-23p19 was significantly higher ($P < 0.001$) in tumors of both IL-12 KO and WT mice than the basal levels of IL-23p19 in the skin samples of the corresponding non-UVB-exposed control mice (Fig. 6B). Moreover, the expression level of mRNA of IL-23p19 was significantly higher ($P < 0.01$) in the tumors of IL-12 KO mice than the tumors of their WT mice.

Discussion

We had found previously that UVB-induced tumors of C3H/HeN mice express high levels of angiogenic factors, such as VEGF, MMP-2, MMP-9, and CD31 (25), compared with non-UVB-exposed normal skin, suggesting that angiogenesis plays a role in the development of UVB-induced tumors. In a murine model of breast cancer, IL-12 has been shown to exert a potent antiangiogenic effects, which contribute to tumor regression (16, 33). In this breast cancer model, on treatment with IL-12, the levels of VEGF and MMP-9 in the tumors declined and the tumors regressed (33). Our current analysis of tumor development in IL-12-deficient mice exposed to a photocarcinogenesis protocol confirmed our previous data (12) that indicated that the size of the tumors in IL-12-deficient mice was greater than that of the UVB-induced tumors in their WT counterparts. We have now established that the tumor vasculature is more extensive in the UVB-induced tumors of the IL-12 KO mice than the UVB-induced tumors of WT mice, indicating that the more aggressive growth of the UVB-induced tumors in the IL-12 KO mice is associated, at least in part, with enhanced angiogenesis. Moreover, the expression of molecules that

are associated with neovascularization or the promotion of angiogenesis, including, CD31, VEGF, bFGF, MMP-2, MMP-3, MMP-7, and MMP-9, were significantly higher in the UVB-induced tumors of IL-12 KO mice. Thus, IL-12 seems to inhibit UVB-induced tumor growth, at least in part, through its inhibition of angiogenesis. Further, IFN- γ has been associated with the reduction in angiogenesis. As IL-12 stimulates the secretion of IFN- γ , the absence of IL-12 in IL-12 KO mice obviously would reduce the levels of IFN- γ in IL-12 KO mouse skin and therefore may play a role in enhancement of tumor angiogenesis in IL-12 KO mice; however, it remains to be verified.

Our current analysis of tumor development in IL-12-deficient mice exposed to a photocarcinogenesis protocol also confirmed that the incidence and multiplicity of the tumors was greater in the IL-12-deficient mice than their WT counterparts. We have shown previously that irradiation of the mouse skin with a single exposure of UVB enhances the level of IL-12 in the skin and draining lymph nodes (34) compared with the levels of IL-12 in non-UVB-exposed mice. When compared with the effects of a single UVB exposure, chronic exposure to UVB for several weeks results in lesser enhancement of the levels of IL-12 in mice. As the levels of IL-12 are decreased in WT mice after chronic exposure to UVB irradiation, we can assume that this is most likely the reason that there is only a 15% difference (increase) in tumor incidence in IL-12 KO mice compared with their WT counterparts. It is known that exposure of the skin to UVB induces DNA damage, which is primarily in the form of the generation of cyclobutane pyrimidine dimers (CPD). The formation of CPDs has been implicated in UVB-induced immunosuppression and initiation of photocarcinogenesis. The nucleotide excision repair (NER) mechanism has the ability to repair CPDs and thus may prevent photocarcinogenesis. We, and others, have shown that IL-12 has the capacity to repair UVB-induced DNA damage in the form of CPDs through the NER mechanism (12, 24, 35). We have shown that, after UV irradiation, WT mice remove or repair UV-induced CPDs faster than IL-12 KO mice. This is in concordance with the greater susceptibility of IL-12 KO mice than WT mice to photocarcinogenesis. We have found that the NER capacity of IL-12

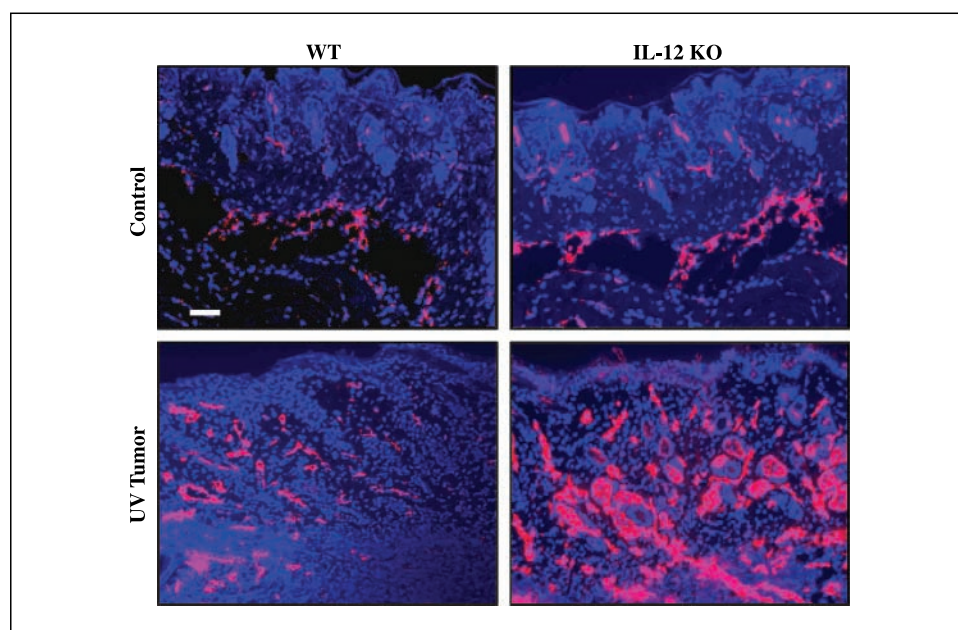


Figure 4. UVB exposure induces higher expression of CD31 in skin tumors. The expression level of CD31 in UVB-induced tumors was greater in IL-12 KO mice (right) compared with their WT counterparts (left). Samples of tumors and age-matched normal mouse skin were used for CD31 fluorescence staining. Representative examples of micrographs of staining for CD31 from WT (left) and IL-12 KO (right) mice from experiments conducted in skin or tumor samples from at least six mice which showed identical patterns. CD31-positive staining is indicated by red fluorescence. Bar = 50 μ m.

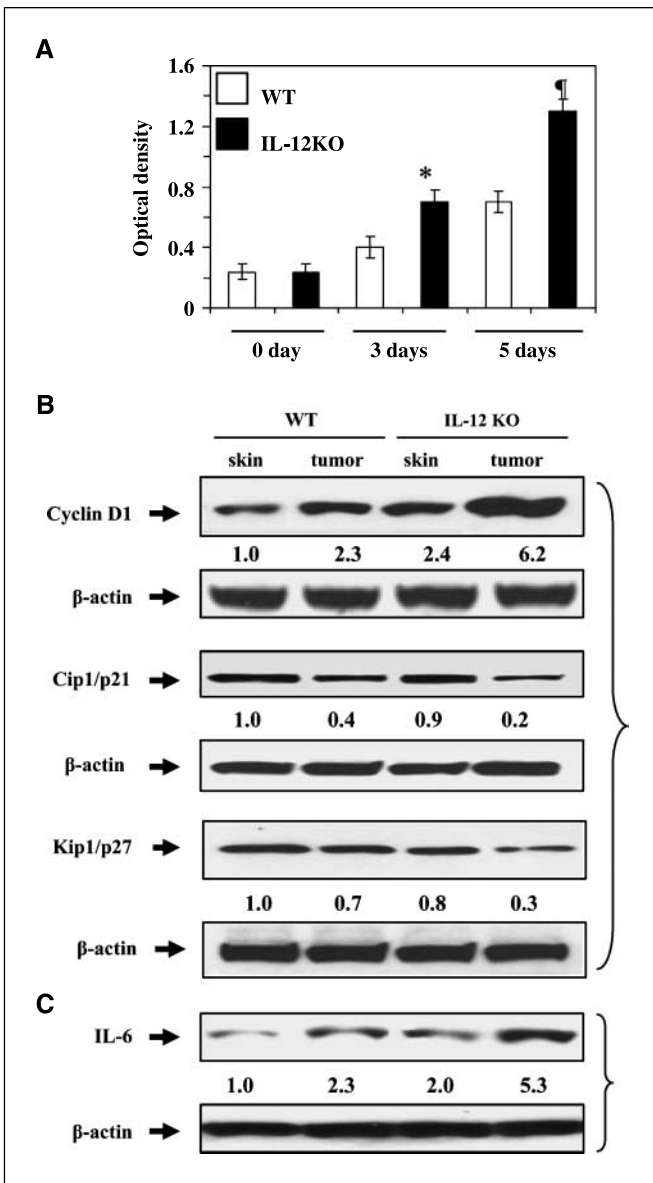


Figure 5. Proliferation capacity of tumor cells from UVB-induced skin tumors. *A*, tumor cells were obtained from tumors induced by UVB in either IL-12 KO or WT mice and subjected to MTT assay immediately (0 day), 3 or 5 days after putting them in culture. Proliferative potential of tumor cells is expressed in terms of absorbance of each sample. *Columns*, mean ($n = 6$); *bars*, SD. *, $P < 0.05$; †, $P < 0.01$, significant difference versus WT. Skin or tumor lysates from WT or IL-12 KO mice were subjected to Western blot analysis to determine the expression of cyclin D1, Cip1/p21, and Kip1/p27 (*B*), and IL-6 (*C*). Representative blot from independent experiments conducted with six tumors from different animals in each treatment group with identical observations. Data were compared with the skin samples from age-matched non-UVB-exposed control mice. The equivalent protein loading was confirmed by probing stripped blots for β -actin. The densitometric data (arbitrary) of each band of the blot are shown under the immunoblots.

KO mice is normal. On s.c. injection of recombinant IL-12 into the UV-irradiated skin of IL-12 KO mice, the repair of UVB-induced CPDs was enhanced when compared with the level of repair in UVB-exposed skin of IL-12 KO mice that was treated with a control injection. Thus, we believe that the expression of NER genes is unaffected and remains intact or normal in IL-12 KO mice.

The formation of UVB-induced sunburn cells is primarily a consequence of DNA damage. We have observed a significant

reduction in the numbers of sunburn cells at 24 and 48 h after UV irradiation compared with the numbers at 10 h after UVB irradiation in WT mice. In IL-12 KO mice, however, this spontaneous reduction in the number of sunburn cells was significantly slower and, at each time point studied, was less than that observed in WT mice (12). S.c. administration of recombinant IL-12 to UVB-irradiated IL-12 KO mouse skin resulted in a significantly lower percentage of sunburn cells at 24 and 48 h after UVB irradiation than in control, sham-treated UVB-irradiated IL-12 KO mouse skin. These observations suggest that the skin cells in IL-12 KO mice are more sensitive to UV radiation in terms of UV-induced DNA damage and their repair than WT mice, and this may be the reason that IL-12 deficiency enhances photocarcinogenesis in mice.

We also found that the expression levels of MMPs and VEGF were higher in the UVB-exposed skin of IL-12 KO mice than in the UVB-exposed skin of their WT counterparts, suggesting that IL-12 may act to inhibit the early development of neovascularization that may occur before overt development of tumors. This may contribute to the higher incidence and larger growth of the tumors in the IL-12 KO mice; however, these molecules also act to promote tumor development through mechanisms other than the promotion of

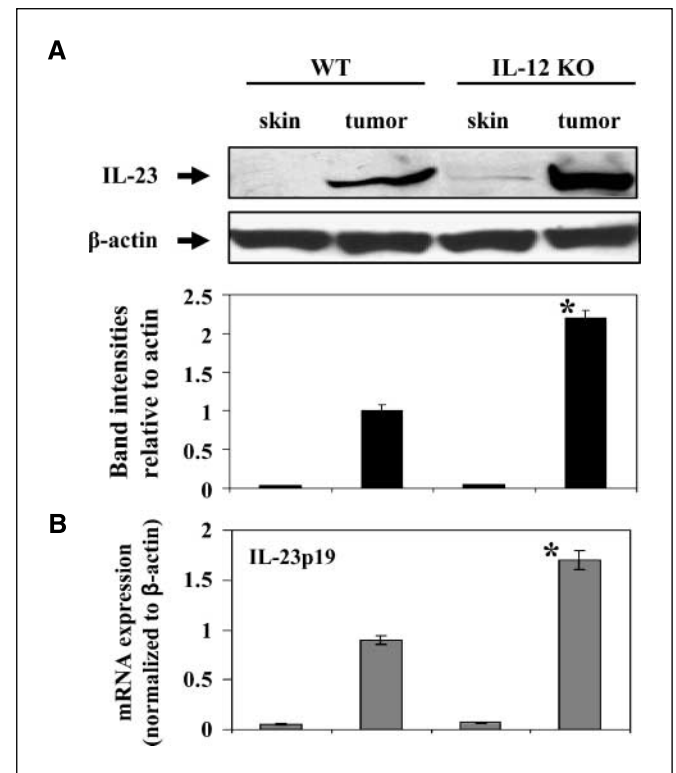


Figure 6. UVB-induced skin tumors express higher levels of IL-23 protein and mRNA in tumors of IL-12 KO mice than WT. *A*, skin and tumor lysates from WT or IL-12 KO mice were subjected to Western blot analysis to determine the expression of IL-23. Representative blot from independent experiments conducted in tumors or skin samples from 10 different animals in each treatment group with identical observations. Equivalent protein loading was confirmed by probing stripped blots for β -actin. *B*, the level of IL-23p19 mRNA expression was quantitated using real-time PCR SYBR Green system as described in Materials and Methods. The results are presented as the expression of the IL-23p19 mRNA with normalization to β -actin using the C_t method. *Columns*, mean from skin or tumor samples from six different animals in each treatment group; *bars*, SD. *, $P < 0.01$, significant difference versus WT.

angiogenesis. For example, MMPs can promote tumorigenesis through their effects on differentiation, apoptosis, invasion, and metastasis through their ability to degrade many components of the extracellular matrix as well as by promoting angiogenesis (36–38).

Human and murine squamous cell carcinomas have been reported to produce proinflammatory cytokines, including IL-1 α , IL-6, and IL-8. Production of these cytokines promotes a suitable microenvironment for angiogenesis and tumor progression in a variety of neoplasms (39). We found that IL-12 deficiency enhanced the up-regulation of IL-6 in tumors. IL-6 has been reported to induce MMPs, which by themselves promote angiogenesis and invasion by acting on extracellular matrix proteins (40). Thus, it seems that enhanced expression and higher activity of MMPs in conjunction with IL-6 contribute to the more aggressive growth behavior of the tumors generated in IL-12 KO mice. We also found that IL-12 deficiency enhanced the expression of another proinflammatory cytokine, IL-23, in UVB-induced tumors. It has been reported that IL-23 promotes tumor incidence and growth and that it is overexpressed in human cancers of various organs (32). It has been shown to promote inflammatory responses, such as up-regulation of the MMP-9, and to enhance angiogenesis. The induction of IL-23–derived processes leads to the pathogenesis of several immune-mediated inflammatory diseases (30). IL-23 shares a common subunit with IL-12. Thus, we speculate that the association of IL-12 deficiency with up-regulation of IL-23 may suggest a key molecular link by which IL-12 regulates the UVB-induced proinflammatory and angiogenic responses; however, further analysis of the role of IL-23 in photocarcinogenesis is required.

It should be noted that analysis of UVB-induced tumor cells *in vitro* using a MTT assay and analysis of the expression of cyclin D1 suggested that cells obtained from established tumors from IL-12–deficient mice had a higher proliferative capacity than cells obtained from established tumors from WT mice. Schwarz et al. (35) conducted a clonogenic survival assay with skin tumor cells obtained from IL-12 KO mice and their WT counterparts. They observed that the number of colonies increased with time when tumor cells obtained from IL-12 KO mice and WT mice were used; however, the frequency of colonies was much higher when tumor cells obtained from IL-12 KO mice were used than when tumor cells from WT mice were used. These observations support the evidence that higher proliferative potential of tumor cells in IL-12 KO mice may have contributed faster and larger tumor growth in

these mice. This may also suggest that IL-12 deficiency has a direct effect on the behavior of tumor cells, independent of the effects on the microenvironment. In addition to the enhanced level of cyclin D1 in the tumors of IL-12 KO mice than WT, we have checked and compare the levels of cell cycle regulatory or inhibitory proteins that have roles in controlling the proliferation of cells, in IL-12 KO and WT mice. We have found that cell cycle checkpoints that we have tested through this approach, and particularly the levels of cell cycle inhibitory proteins (Cip1/p21 and Kip1/p27), are intact in IL-12 KO mice and their levels are not significantly different with those in WT mice. However, on comparison of the levels of Cip1/p21 and Kip1/p27 proteins in tumor samples compared with normal skin samples, we found a much greater reduction in the IL-12 KO mice than in the corresponding WT mice. This suggests that the rate of proliferation of tumor cells is not as well controlled in IL-12 KO mice than in WT mice, which may result in the more rapid growth of tumors in IL-12 KO and their larger size. These results also indicate that the cell cycle regulatory checkpoints are more susceptible to UV irradiation in the IL-12 KO mice than the WT mice.

Taken together, our data indicate for the first time that the deficiency of IL-12 in mice promotes the proangiogenic stimulus of UV radiation that leads to the stimulation of UV-induced skin carcinogenesis. These data are consistent with the reports that IL-12 has the ability to cure or improve the survival of tumor-bearing mice and is associated with the enhancement of *in vivo* antitumor immune responses and antitumor activity in several other tumor models (7, 11, 15), with the presence of IL-12 at the tumor site being critical for tumor regression (11). As endogenous production of IL-12 may inhibit UVB-induced skin carcinogenesis, it is tempting to speculate that the stimulation of IL-12 in *in vivo* system by any means, such as through dietary supplements, topical treatments, or IL-12 therapy, may prove efficacious in the prevention and treatment of solar UV radiation-induced skin cancers in humans.

Acknowledgments

Received 8/23/2006; revised 1/11/2007; accepted 2/14/2007.

Grant support: Veterans Administration Merit Review Award (S.K. Katiyar), National Center for Complementary and Alternative Medicine/NIH grant 1 RO1 AT002536 (S.K. Katiyar), and the University of Alabama at Birmingham Skin Diseases Research Center grant AR050948-01.

The costs of publication of this article were defrayed in part by the payment of page charges. This article must therefore be hereby marked *advertisement* in accordance with 18 U.S.C. Section 1734 solely to indicate this fact.

References

- Katiyar SK, Korman NJ, Mukhtar H, Agarwal R. Protective effects of Silymarin against photocarcinogenesis in a mouse skin model. *J Natl Cancer Inst* 1997; 89:556–66.
- Katiyar SK. Oxidative stress and photocarcinogenesis: strategies for prevention. In: Singh KK, editor. *Oxidative stress, disease, and cancer*. London: Imperial College Press; 2006, p. 933–64.
- Meunier L, Raison-Peyron N, Meynadier J. UV-induced immunosuppression and skin cancers. *Rev Med Interne* 1998;19:247–54.
- Yoshikawa T, Rae V, Bruins-Slot W, van den Berg JW, Taylor JR, Streilein JW. Susceptibility to effects of UVB radiation on induction of contact hypersensitivity as a risk factor for skin cancer in humans. *J Invest Dermatol* 1990;95:530–6.
- Muller G, Saloga J, Germann T, Schuler G, Knop J, Enk AH. IL-12 as mediator and adjuvant for the induction of contact sensitivity *in vivo*. *J Immunol* 1995;155:4661–8.
- Schwarz A, Grabbe S, Aragane Y, et al. Interleukin-12 prevents ultraviolet B-induced local immunosuppression and overcomes UVB-induced tolerance. *J Invest Dermatol* 1996;106:1187–91.
- Brunda MJ, Luistro L, Warriar RR, et al. Antitumor and antimetastatic activity of interleukin-12 against murine tumors. *J Exp Med* 1993;178:1223–30.
- Brunda MJ. Interleukin-12. *J Leukoc Biol* 1994;55:280–8.
- Zou JP, Yamamoto N, Fuzii T, et al. Systemic administration of rIL-12 induces complete tumor regression and protective immunity: response is correlated with a striking reversal of suppressed IFN- γ production by anti-tumor T cells. *Int Immunol* 1995;7: 1135–45.
- Robertson MJ, Ritz J. Interleukin-12: basic biology and potential applications in cancer treatment. *Oncologist* 1996;1:88–97.
- Colombo MP, Vagliani M, Spreafico F, et al. Amount of interleukin 12 available at the tumor site is critical for tumor regression. *Cancer Res* 1996;56:2531–4.
- Meeran SK, Mantena SK, Meleth S, Elmets CA, Katiyar SK. Interleukin-12-deficient mice are at greater risk of ultraviolet radiation-induced skin tumors and malignant transformation of papillomas to carcinomas. *Mol Cancer Ther* 2006;5:825–32.
- Chen L, Chen D, Bloack E, O'Donnell M, Kufe DW, Clinton SK. Eradication of murine bladder carcinoma by intratumor injection of a bicistronic adenoviral vector carrying cDNAs for the IL-12 heterodimer and its inhibition by the p40 subunit homodimer. *J Immunol* 1997;159:351–9.
- Siders W, Wright P, Hixon J, et al. T cell- and NK cell-independent inhibition of hepatic metastases by

- systemic administration of an IL-12-expressing recombinant adenovirus. *J Immunol* 1998;160:5465-74.
15. Nastala CL, Edington HD, McKinney TG, et al. Recombinant IL-12 administration induces tumor-regression in association with IFN- γ production. *J Immunol* 1994;153:1697-706.
 16. Coughlin CM, Salhany KE, Wysocka M, et al. Interleukin-12 and interleukin-18 synergistically induce murine tumor regression which involves inhibition of angiogenesis. *J Clin Invest* 1998;101:1441-52.
 17. Risau W. Differentiation of endothelium. *FASEB J* 1995;9:926-33.
 18. Conti CJ. Vascular endothelial growth factor: regulation in the mouse skin carcinogenesis model and use in antiangiogenesis cancer therapy. *Oncologist* 2002;7:4-11.
 19. Ferrara N, Davis-Smyth T. The biology of vascular endothelial growth factor. *Endocr Rev* 1997;18:4-25.
 20. Alon T, Hemo I, Itin A, Pe'er J, Stone J, Keshet E. Vascular endothelial growth factor acts as a survival factor for newly formed retinal vessels and has implications for retinopathy of prematurity. *Nat Med* 1995;1:1024-8.
 21. Ben-Zamin LE, Golijanin D, Itin A, Podes D, Keshet E. Selective ablation of immature blood vessels in established human tumors follows vascular endothelial growth factor withdrawal. *J Clin Invest* 1999;103:159-65.
 22. Katiyar SK. Matrix metalloproteinases in cancer metastasis: molecular targets for prostate cancer prevention by green tea polyphenols and grape seed proanthocyanidins. *Endocr Metab Immune Disord Drug Targets* 2006;6:17-24.
 23. Mittal A, Elmets CA, Katiyar SK. Dietary feeding of proanthocyanidins from grape seeds prevents photocarcinogenesis in SKH-1 hairless mice: relationship to decreased fat and lipid peroxidation. *Carcinogenesis* 2003;24:1379-88.
 24. Meeran SM, Mantena SK, Katiyar SK. Prevention of ultraviolet radiation-induced immunosuppression by (-)-epigallocatechin-3-gallate in mice is mediated through interleukin 12-dependent DNA repair. *Clin Cancer Res* 2006;12:2272-80.
 25. Mantena SK, Meeran SM, Elmets CA, Katiyar SK. Orally administered green tea polyphenols prevent ultraviolet radiation-induced skin cancer in mice through activation of cytotoxic T cells and inhibition of angiogenesis in tumors. *J Nutr* 2005;135:2871-7.
 26. Vayalil PK, Elmets CA, Katiyar SK. Treatment of green tea polyphenols in hydrophilic cream prevents UVB-induced oxidation of lipids and proteins, depletion of antioxidant enzymes, and phosphorylation of MAPK proteins in SKH-1 hairless mouse skin. *Carcinogenesis* 2003;24:927-36.
 27. Mantena SK, Sharma SD, Katiyar SK. Berberine, a natural product, induces G₁-phase cell cycle arrest and caspase-3-dependent apoptosis in human prostate carcinoma cells. *Mol Cancer Ther* 2006;5:296-308.
 28. Hanahan D, Folkman J. Patterns and emerging mechanisms of the angiogenic switch during tumorigenesis. *Cell* 1996;86:353-64.
 29. Schlaeppi JM, Wood JM. Targeting vascular endothelial growth factor (VEGF) for anti-tumor therapy, by anti-VEGF neutralizing monoclonal antibodies or by VEGF receptor tyrosine-kinase inhibitors. *Cancer Metastasis Rev* 1999;18:473-81.
 30. Langrish CL, McKenzie BS, Wilson NJ, de Waal Malefyt R, Kastelein RA, Cua DJ. IL-12 and IL-23: master regulators of innate and adaptive immunity. *Immunol Rev* 2004;202:96-105.
 31. Oppmann B, Lesley R, Blom B, et al. Novel p19 protein engages IL-12p40 to form a cytokine, IL-23, with biological activities similar as well as distinct from IL-12. *Immunity* 2000;13:715-25.
 32. Langowski JL, Zhang X, Wu L, et al. IL-23 promotes tumour incidence and growth. *Nature* 2006;442:461-5. Epub 2006 May 10.
 33. Dias S, Boyd R, Balkwill F. IL-12 regulates VEGF and MMPs in a murine breast cancer model. *Int J Cancer* 1998;78:361-5.
 34. Katiyar SK, Challa A, McCormick TS, Cooper KD, Mukhtar H. Prevention of UVB-induced immunosuppression in mice by green tea polyphenol (-)-epigallocatechin-3-gallate may be associated with alterations in IL-10 and IL-12 production. *Carcinogenesis* 1999;20:2117-24.
 35. Schwarz A, Stander S, Berneburg M, et al. Interleukin-12 suppresses ultraviolet radiation-induced apoptosis by inducing DNA repair. *Nat Cell Biol* 2002;4:26-31.
 36. Yu AE, Hewitt RE, Connor EW, Stetler-Stevenson WG. Matrix metalloproteinases. Novel targets for directed cancer therapy. *Drugs Aging* 1997;11:229-44.
 37. Chambers AF, Matrisian LM. Changing views of the role of matrix metalloproteinases in metastasis. *J Natl Cancer Inst* 1997;89:1260-70.
 38. John A, Tuszynski G. The role of matrix metalloproteinases in tumor angiogenesis and tumor metastasis. *Pathol Oncol Res* 2001;7:14-23.
 39. Smith CW, Chen Z, Dong G, et al. The host environment promotes the development of primary and metastatic squamous cell carcinomas that constitutively express proinflammatory cytokines IL-1 α , IL-6, GM-CSF, and KC. *Clin Exp Metastasis* 1998;16:655-64.
 40. Sundelin K, Roberg K, Grenman R, Hakansson L. Effects of cytokines on matrix metalloproteinase expression in oral squamous cell carcinoma *in vitro*. *Acta Otolaryngol* 2005;125:765-73.